

## Efficient solution of multiple cracks in great number using eigen COD boundary integral equations with iteration procedure

Hang Ma<sup>a,\*</sup>, Zhao Guo<sup>b</sup>, Manicka Dhanasekar<sup>c</sup>, Cheng Yan<sup>d</sup>, Yijun Liu<sup>e</sup>

<sup>a</sup> Department of Mechanics, College of Sciences, Shanghai University, Shanghai 200444, China

<sup>b</sup> Shanghai Institute of Applied Mathematics and Mechanics, Shanghai University, Shanghai 200072, China

<sup>c</sup> School of Civil engineering and Built Environment, Queensland University of Technology, QLD 4001, Australia

<sup>d</sup> School of Chemistry, Physics and Mechanical Engineering, Queensland University of Technology, QLD 4001, Australia

<sup>e</sup> Mechanical Engineering, University of Cincinnati, Cincinnati, OH 45221-0072, USA

### ARTICLE INFO

#### Article history:

Received 18 September 2012

Accepted 30 December 2012

#### Keywords:

Multiple cracks

Eigen COD

Boundary integral equation

Local Eshelby matrix

Iteration

Stress intensity factor

### ABSTRACT

A newly developed computational approach is proposed in the paper for the analysis of multiple crack problems based on the eigen crack opening displacement (COD) boundary integral equations. The eigen COD particularly refers to a crack in an infinite domain under fictitious traction acting on the crack surface. With the concept of eigen COD, the multiple cracks in great number can be solved by using the conventional displacement discontinuity boundary integral equations in an iterative fashion with a small size of system matrix to determine all the unknown CODs step by step. To deal with the interactions among cracks for multiple crack problems, all cracks in the problem are divided into two groups, namely the adjacent group and the far-field group, according to the distance to the current crack in consideration. The adjacent group contains cracks with relatively small distances but strong effects to the current crack, while the others, the cracks of far-field group are composed of those with relatively large distances. Correspondingly, the eigen COD of the current crack is computed in two parts. The first part is computed by using the fictitious tractions of adjacent cracks via the local Eshelby matrix derived from the traction boundary integral equations in discretized form, while the second part is computed by using those of far-field cracks so that the high computational efficiency can be achieved in the proposed approach. The numerical results of the proposed approach are compared not only with those using the dual boundary integral equations (D-BIE) and the BIE with numerical Green's functions (NGF) but also with those of the analytical solutions in literature. The effectiveness and the efficiency of the proposed approach is verified. Numerical examples are provided for the stress intensity factors of cracks, up to several thousands in number, in both the finite and infinite plates.

© 2013 Elsevier Ltd. All rights reserved.

### 1. Introduction

Quite a lot of brittle or quasi-brittle materials [1–4] can be modeled as solids with multiple cracks where the presence of cracks is a common reason for failures of these materials, such as concretes, rocks, ceramics, brittle metallic materials, as well as the fibre-reinforced brittle materials after certain extent of tensile damage. The prediction of crack behavior represents a real concern among engineers designing general structures and has always been a challenge for researchers. There are also many researches reported in literature, showing the significance of this kind of research. It is true that the exact locations of the cracks are difficult to know, just like those of multiple particles in solids. This would be one of the reasons of scatters of properties such as fracture

strengths observed from the brittle materials owing partially to the distributions of cracks in sizes, locations, orientations and interactions among cracks, which are challenge tasks and need to be investigated. Since Irwin postulated that crack behavior is determined only by the value of the stress intensity factor (SIF) which depends on the stress field accuracy in the vicinity of the crack tip, the SIF are the main parameters to seek in linear elastic fracture mechanisms (LEFM). Due to their complexity, most crack problems cannot be solved by analytical procedures [5]. The appropriate numerical modeling of LEFM problems became also a challenge for engineers. There are generically two numerical modeling difficulties specifically to the boundary element method (BEM) [6], i.e., the accurate determination of the stress field near the crack tip and the degeneration of the integral equation because of the geometric coincidence of crack surfaces. A good refinement of the mesh associated to the usage of special tip elements are usually enough to overcome the first difficulty [7] while the degeneration in the BEM is usually avoided by applying the sub-region technique

\* Corresponding author. Tel.: +86 21 56139177; fax: +86 21 66134080.  
E-mail address: [hangma@staff.shu.edu.cn](mailto:hangma@staff.shu.edu.cn) (H. Ma).

[8,9]. One of the established alternatives to the degeneration problem is the simultaneous utilization of the traditional displacement and the traction integral equations, known as mixed or dual formulation of boundary integral equations (BIE) [10,11]. However, for the multiple crack problems, the size of the system matrix of the dual BIE will grow very large with the increase of the number of cracks since the unknowns appear on both the crack surfaces and outer boundaries of the problem. It seems that the mathematical techniques of the fast multipole expansions [12,13] should be employed to deal with such a large scale problem so that the solution complexity increases.

One of the most accurate solutions obtained for this class of problems, though restricted in its analytical form, involves the usage of analytical Green's functions, i.e., the Erdogan function, for a cracked medium, as the fundamental solution in the BEM [14] to eliminate the unknowns at crack surfaces. The integration along the crack surface is necessary only when prescribed tractions exist. Since the analytical Green's functions are often in complex form, limited to the two-dimensional problems and to a single crack of simple shape, not available for the majority of applications especially for three-dimensional problems, the numerical Green's function (NGF) procedure suggested by Telles [15,16] has gained attention as an efficient option to solve LEFM engineering problems to avoid the crack tip discretization.

In the Telles method, the numerical Green's function can be written in terms of a superposition of a full space fundamental solution plus a complementary part which provides satisfaction of the traction free requirement over the crack surfaces. The hyper-singular boundary integral equation is used to obtain the crack surface fundamental displacement discontinuities numerically for the complementary problem, i.e., the problem where the crack, embedded in the infinite medium, is loaded with the negative of the Kelvin tractions [15,16]. Therefore, once the fundamental displacement discontinuities for the cracks are known, the complementary numerical solution of the NGF for displacements and tractions, at any point inside the multi-cracked infinite domain, is obtained directly by using the classical and traction boundary integral equations. In this way, the final fundamental Green's function kernel combines the two effects: the Kelvin analytical kernels and the complementary numerical ones [15,16]. The procedure automatically includes the cracks into the fundamental numerical Green's function and, therefore, the classical BEM can be used, without having to define boundary elements over the cracks, to determine the external boundary unknowns of the proposed problem. In consequence, the system matrix of the problem remains of small scale and the SIF needed can be computed.

For the multiple crack problems, however, the size of the matrix to determine the complementary solutions of the NGF will also grow very large with the increase of the number of cracks since the complementary solutions have to be determined numerically during the problem solution using the BEM. Kachanov [17,18] proposed a method very popular in practice to deal with the interaction problems based on the superposition technique and the assumption that only average tractions on individual cracks contribute to the interaction effect [19]. To eliminate these shortcomings, the concept of the eigen crack opening displacements (COD) are firstly introduced in [20] and reaffirmed in the present paper, which can be defined as the crack opening displacement of a crack in infinite domain under the fictitious traction acting on crack surface. With the concept of eigen COD, the multiple crack problem can be solved by using the conventional displacement discontinuity boundary integral equations with a small size of system matrix but in an iterative fashion because of the interactions among multiple cracks.

To deal with the interaction effects more efficiently in the present work but without the Kachanov's assumption, the

superposition technique is employed by dividing all cracks into two groups according to the distances of cracks to the current crack. The cracks of adjacent group are characterized by relatively small distances and strong effects to the current crack, while the others, the cracks of far-field group are characterized by relatively large distances. Correspondingly, the eigen COD of the current crack is computed using two parts. The first part is computed by using the fictitious tractions of adjacent cracks via the local Eshelby matrix derived from the traction boundary integral equations in discretized form, while the second part is computed by using those of far-field cracks. In the proposed approach, dividing cracks into two groups according to the distances to the current crack is the key factor and the main improvement of the previous work [20] to deal with the interactions among cracks because the interactions depend on the distances of cracks so that the high computational efficiency can be achieved, just like those of the computational model in the eigenstrain BIE for the multiple inclusion problems [21,22].

In the present paper, the fracture mechanics problems in plane elasticity are considered and solved numerically using the boundary point method (BPM), a discretized form of the BIE [23,24]. In Section 2, the basic equations and the local Eshelby matrix are introduced with numerical treatments in the computational model of eigen COD boundary integral equations. The solution procedures are given in Section 3 with the iteration details and the convergence criterion. In Section 4, the numerical examples are presented. The stress intensity factors (SIFs) of the multiple crack problems in the finite and infinite plates are solved with the proposed approach, the eigen-COD boundary integral equations with the iteration procedure. The numerical results in the finite plates are compared with those using the dual boundary integral equations (D-BIE) [10,11] and the BIE with the numerical Green's function (NGF) [15,16] and as well as with those in literature. The numerical results in the infinite plates are compared with the analytical solutions in literature. In order to show the present work carried on, an Appendix A is attached to explain how the terminology 'eigen COD' comes from and how the formulation of the eigen COD BIE correlates with that of the eigenstrain BIE.

## 2. Eigen COD boundary integral equations

### 2.1. Basic formulations

Consider an elastic domain  $\Omega$  with boundary  $\Gamma$  containing multiple  $N_c$  cracks. The displacements at the source point  $y$  can be expressed by the displacement BIE with the displacement discontinuities, or the COD on crack surfaces,  $A_m$ , as follows [15,16,25]:

$$\begin{aligned} \gamma u_i(y) = & \int_{\Gamma} \tau_j(x) u_{ij}^*(x, y) d\Gamma(x) - \int_{\Gamma} u_j(x) \tau_{ij}^*(x, y) d\Gamma(x) \\ & - \sum_{m=1}^{N_c} \int_{A_m^+} \Delta u_j(x) \tau_{ij}^*(x, y) dA(x), \quad y \in (\Gamma \cup \Omega) \setminus A_m, \quad (m = 1, \dots, N_c) \end{aligned} \quad (1)$$

where  $u_{ij}^*$  and  $\tau_{ij}^*$  are the displacement and the traction fundamental solutions, respectively [6,10].  $x$  is the field point.  $\gamma = 1$  if  $y \in \Omega$  and  $\gamma = 0.5$  if  $y \in \Gamma$  where  $\Gamma$  is smooth.  $\Delta u_i$  are the displacement discontinuities, or the COD at the surfaces of multiple cracks defined by

$$\Delta u_i(x) = u_i(x)|_{x \in A^+} - u_i(x)|_{x \in A^-} \quad (2)$$

where  $A^+$  and  $A^-$  represent the upper and the lower surfaces of the crack. It is clear that if all the CODs are known, the multiple crack problem can be solved by Eq. (1) in discrete form such as the BEM [6] without the crack discretization [15]. The stresses

and tractions at the point  $y$  can be computed by the stress BIE and the traction BIE, respectively, with the displacement discontinuities of multiple cracks as follows:

$$\begin{aligned} \gamma\sigma_{ij}(y) &= \int_{\Gamma} \tau_k(x)u_{ijk}^*(x,y)d\Gamma(x) - \int_{\Gamma} u_k(x)\tau_{ijk}^*(x,y)d\Gamma(x) \\ &\quad - \sum_{m=1}^{N_c} \int_{A_m^+} \Delta u_k(x)\tau_{ijk}^*(x,y)dA(x), \quad y \in (\Gamma \cup \Omega) \setminus (\cup A_m) \end{aligned} \quad (3)$$

$$\begin{aligned} \gamma\tau_i(y) &= n_j(y) \int_{\Gamma} \tau_k(x)u_{ijk}^*(x,y)d\Gamma(x) - n_j(y) \int_{\Gamma} u_k(x)\tau_{ijk}^*(x,y)d\Gamma(x) \\ &\quad - n_j(y) \sum_{m=1}^{N_c} \int_{A_m^+} \Delta u_k(x)\tau_{ijk}^*(x,y)dA(x), \quad y \in (\Gamma \cup \Omega) \setminus (\cup A_m) \end{aligned} \quad (4)$$

where  $n_j$  represents the unit directional cosine at  $y$ . Correspondingly, Eqs. (1), (3) and (4) are named as the eigen COD boundary integral equations [20] where the last term in Eq. (1) can be derived from the domain integrals in the formulation of eigen-strain BIE [21,22] as shown in Appendix A. However, it needs to be pointed out that all the CODs are unknown in this form of the conventional displacement discontinuity boundary integral equations. In the present work, the CODs are to be determined step by step with the aid of the concept of eigen COD and the local Eshelby matrix, which will be discussed in what follows.

### 2.2. Eigen COD

Consider a traction-free crack  $A$  having a COD response in infinite domain under the far-field loading  $\sigma$  as shown in Fig. 1a, which can be decomposed equivalently into two cases: an enclosed crack without COD response under both the actions of the tractions with a minus sign along its surface and the far-field loading (Fig. 1b) and an opened crack having the same COD response as that of case (a) under the fictitious tractions presumably applied on its surface without the far-field loading (Fig. 1c). It needs to be pointed out that in the framework of the BIE, the fictitious tractions can be computed numerically using Eq. (4) without difficulty along this crack surface regardless of the existence of crack. The eigen COD,  $\Delta u_i$ , can be defined as the crack opening displacement of the crack  $A$  in infinite domain under the fictitious traction,  $\tau_i$ , acting on its surface.

If there is only one crack to be considered, after a limiting process, the COD and the traction of the single crack in infinite plate can be correlated with each other using the hypersingular traction BIE derived from Eq. (4) in the global coordinate as follows by placing the point  $y$  into the crack surface [20]:

$$n_j(y)\text{HFP} \int_{A^+} \Delta u_k(x)\tau_{ijk}^*(x,y)dA(x) = -\tau_i(y) \quad y \in A^+ \quad (5)$$

where HFP means the Hadamard finite part. Consider the case of a straight crack and noticed the fact of the similarity between the two loading modes [15], the opening and the sliding, Eq. (5) can be reduced into the following simplified form supposing the unit crack length of  $2a$  ( $a=1$ ):

$$\frac{\mu}{2\pi(1-\nu)} \text{HFP} \int_{-1}^{+1} \frac{\delta_i}{r^2(x,y)} dA(x) = -\tau_i(y) \quad (6)$$

where  $\mu$  and  $\nu$  are, respectively, the shear modulus and Poisson's ratio of the material,  $r$  the distance between  $x$  and  $y$ .  $\delta_i$  in Eq. (6) stand for the COD. For the simple case of tractions such as constant and linear distributions, the analytical solutions of COD are available in the literature [26]. For the general case, the COD can be solved numerically. By dropping the subscript  $i$  in Eq. (6) and employing the explicit expression for the HFP integrals [27] and choosing the collocation points  $j$  to be the same ones at the Gauss stations  $k$ , the discrete form of Eq. (6) can be derived as follows in the local coordinate:

$$\begin{aligned} \frac{\mu}{2\pi(1-\nu)} \left\{ \sum_{j=1, j \neq k}^{N_G} \frac{w_j}{(\xi_j - \xi_k)^2} \delta_j - \left[ \sum_{j=1, j \neq k}^{N_G} \frac{w_j}{(\xi_j - \xi_k)^2} + \frac{2}{1 - \xi_i^2} \right] \delta_k \right. \\ \left. - \left[ \sum_{j=1, j \neq k}^{N_G} \frac{w_j}{\xi_j - \xi_k} \ln \left( \frac{1 - \xi_k}{1 + \xi_i} \right) \right] \frac{\partial \delta_k}{\partial \xi} + \frac{w_k}{2} \frac{\partial^2 \delta_k}{\partial \xi^2} \right\} = -\tau_k, \quad k = 1, \dots, N_G \end{aligned} \quad (7)$$

where  $w_j$  and  $\xi_j$  are, respectively, the Gauss weights and stations and  $N_G$  the total Gauss number. In order to compute the derivatives of the COD in Eq. (7), a Lagrange polynomial interpolation can be used. Thus

$$\delta = \sum_{k=1}^{N_G} l_k \delta^k \quad (8)$$

where  $l_k$  represent the Lagrange polynomials of order  $N_G + 2$  which are chosen to make the expression (8) satisfy that  $\delta(-a) = \delta(+a) = 0$ . Rewrite (7) in matrix form for both the two modes of opening and sliding as

$$a^{-1} \mathbf{S}^0 \delta = \tau, \quad \mathbf{S}^0 = \begin{bmatrix} \mathbf{S} & \mathbf{0} \\ \mathbf{0} & \mathbf{S} \end{bmatrix} \quad (9)$$

to compute the eigen COD in vector form,  $\delta$ , with the size of  $2N_G \times 1$  by the fictitious traction  $\tau$  with the size of  $2N_G \times 1$  for the crack with the length  $2a$ , where the constant square matrix  $\mathbf{S}$  with the size of  $N_G \times N_G$  is the discretized form of Eq. (7), which can be named as the basic crack matrix for elastostatics.

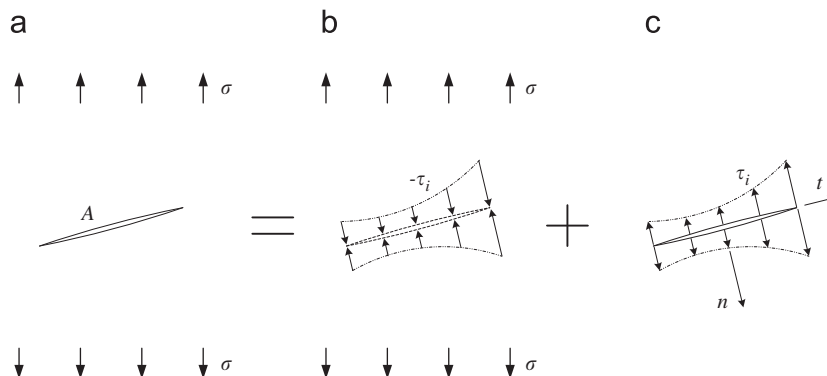


Fig. 1. Fictitious tractions on crack surface.

2.3. Local Eshelby matrix

For the multiple cracks problem as shown in Fig. 2, consider one of the cracks,  $A$ , as the current crack. The fictitious tractions on the crack  $A$  are generated not only by the far-field loading but also affected by all other cracks in the domain, which is the well known interactions among cracks. In the NGF approach [15,16], the interactions of all cracks are considered simultaneously so that the size of the matrix for computing NGF would grow very large with the increase of the number of cracks.

To deal with the interactions among cracks for multiple crack problems, while keeping the computing complexity within a limited range acceptable for running the program on an ordinary desktop computer in the present work, all cracks are divided into two groups according to the non-dimensional radial distances of cracks to the center of the current crack. The cracks of adjacent group, being placed in a circle in dashed-line around the center of the crack  $A$ , are defined as those with relatively small distances to but having strong effects on the current crack  $A$  as shown in Fig. 2. While the others, the cracks of far-field group are defined as those with relatively large distances located outside the circle. It is obvious that in general, the cracks of adjacent group are unique for every current crack of all the cracks in the domain once the radius of the circle in dashed line (Fig. 2) is defined. If there is only one crack in the adjacent group when the radius of the circle is chosen small enough, the problem of relatively sparsely populated cracks can be treated properly owing to the interactions among cracks, which is the case in the previous work [20].

In an infinite space, consider only the cracks in adjacent group of the current crack, place the point  $y$  on the crack surface and denote the number of the cracks of adjacent group as  $N_L$ , Eq. (4) can be written as:

$$n_j(y) \text{HFP} \int_{A_1^+} \Delta u_k(x) \tau_{ijk}^*(x,y) dA(x) + n_j(y) \sum_{m=1, m \neq l}^{N_L} \int_{A_m^+} \Delta u_k(x) \tau_{ijk}^*(x,y) dA(x) = -\tau_i(y), \quad y \in A_l \quad (10)$$

In this way, the eigen COD and the corresponding fictitious tractions are correlated in Eq. 10 for only the cracks of adjacent group irrespective tentatively of the effects of far-field group. The first integral in the left hand side of Eq. (10) is hypersingular having the same structure with that of Eq. (6) which can be computed using Eq. (7). The second integral in the left hand side of Eq. (10) is regular without any difficulty in computing. Writing in matrix form after discretization,

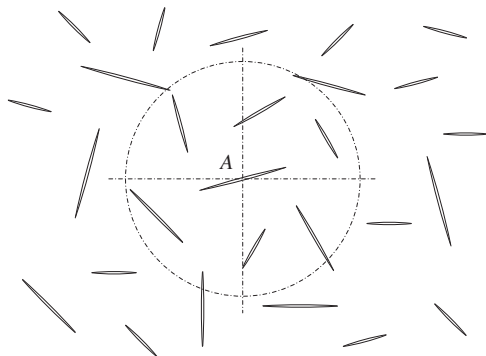


Fig. 2. The group definitions for multiple cracks.

Eq. (10) becomes

$$\begin{bmatrix} a_1^{-1} \mathbf{S}^0 & \mathbf{S}_{12} & \cdots & \mathbf{S}_{1,N_L} \\ \mathbf{S}_{21} & a_2^{-1} \mathbf{S}^0 & & \mathbf{S}_{2,N_L} \\ \vdots & & \ddots & \vdots \\ \mathbf{S}_{N_L,1} & \mathbf{S}_{N_L,2} & \cdots & a_{N_L}^{-1} \mathbf{S}^0 \end{bmatrix} \begin{Bmatrix} \delta_1 \\ \delta_2 \\ \vdots \\ \delta_{N_L} \end{Bmatrix} = \begin{Bmatrix} \tau_1 \\ \tau_2 \\ \vdots \\ \tau_{N_L} \end{Bmatrix} \quad (11)$$

where  $a_k$  are the half length of each crack, the off-diagonal terms  $\mathbf{S}_{km}$  are sub-matrices derived from the discrete form corresponding to the regular integrals in the left hand side of Eq. (10). In fact, the structure of the total square matrix in Eq. (11) is exactly the same with that used in the NGF approach [15,16]. However, there are two distinct differences to be addressed here. The first lies in that in the NGF approach, the matrix should involve all the cracks in the domain in consideration, resulting in a huge size of the matrix while in the present approach, the matrix contains only the cracks of the adjacent group leading to a small size. The second is that in the NGF approach, the fictitious tractions are generated by a unit point force at the source point and the resultant COD are used to compute the displacements at the field point, the complementary part of the NGF, embedded into the fundamental solutions in the overall boundary integral equation to be solved. While in the present approach, the fictitious tractions are generated either by far-field loading in infinite domain or by the boundary loads in finite domains. The resultant COD, the eigen COD, are computed step by step in an iterative procedure to be discussed later and employed for the final results at the convergence. The eigen COD of the  $k$ th current crack, the concerned crack, can be computed by inverting the total square matrix in Eq. (11) then reducing it to obtain

$$\delta_{(k)} = \mathbf{S}_k \tau_{(k)}, \quad k = 1, 2, \dots, N_C \quad (12)$$

where the vector  $\tau_{(k)} = \{\tau_1, \tau_2, \dots, \tau_{N_L}\}_k^T$  with a size of  $(2N_G \times N_L) \times 1$  are the fictitious tractions of all cracks in the adjacent group. The vector  $\delta_{(k)}$  with a size of  $2N_G \times 1$  are the eigen COD of the current crack.  $\mathbf{S}_k$  is reduced from the inverse matrix of the total square matrix at the left hand side of Eq. (11). In the present work,  $\mathbf{S}_k$  is named as the local Eshelby matrix whose size is  $2N_G \times (2N_G \times N_L)$  supposing that the same number of Gauss points is employed for all the cracks in the adjacent group. The local Eshelby matrix can be considered just as the discrete form correlating the fictitious tractions of cracks in adjacent group and the COD of the current crack in infinite plate, derived from the hypersingular boundary integral (10). In general, the local Eshelby matrices are all distinct for every crack in the domain once the radius of the circle in dashed line (Fig. 2) is defined but they are all constant depending only on the local geometries of cracks chosen for the adjacent group and the number of Gauss points adopted so that they need to be computed only once. Nevertheless, for a given multiple cracks problem, there are as many local Eshelby matrices with small sizes as the total number of cracks to be solved. However, from the computational point of view, solving a problem with many small matrices would be much efficient than that of solving a single huge matrix. More the number of cracks involved, much greater the difference of efficiencies between the two problems will be.

In this way, the eigen COD of the current crack should consist of two parts. The first part can be computed by using the fictitious tractions of adjacent cracks with the aid of the local Eshelby matrix using Eq. (12), while the second part can be computed by using those of far-field cracks so that the high computational efficiency can be achieved in the proposed approach. To determine the radius of the circle in dashed line (Fig. 2) defining the size of the near-field group should consider the density or sparsity of cracks in concern, because the interaction among cracks is dependent of the non-dimensional distances normalized by the

current crack size. It is true that if only the cracks in the adjacent group exist in an infinite domain, the CODs and the corresponding fictitious tractions for the cracks of the adjacent group correlate exactly by Eq. (10) or correlate approximately by Eshelby matrix in (12), reflecting relatively strong interactions among cracks to the current crack. While the relatively weak effects of cracks to the current crack in far-field group are treated in the iteration procedures, which is considered to be a key improvement to the previous work [20].

2.4. Stress intensity factors

Owing to that the existence of the definite correlations among the COD, the fictitious traction and the stress intensity factor (SIF) of a crack, in the present work, the SIFs are computed by using the fictitious tractions to avoid the computation of stresses or displacements near crack tips as is conventionally done [7,8,14–16]. First, by defining, respectively, the normal direction as  $n$  (the opening mode) and the tangential direction (the shear mode) as  $t$  with respect to the crack in the local coordinate (Fig. 1c), the fictitious tractions in either direction can be fitted approximately by the polynomial of order  $N_p$  in the local coordinates as follows using the nodal values at Gauss points:

$$\tau = c_0 + c_1 \frac{\eta}{a} + c_2 \left(\frac{\eta}{a}\right)^2 + \dots + c_{N_p} \left(\frac{\eta}{a}\right)^{N_p}, \quad \eta \in [-a, a] \tag{13}$$

where  $c_i$  are the coefficients of the polynomial to be determined. Then the SIF at the two tips of a crack can easily be computed analytically [26] after some derivations using the coefficients,  $c_i$ , of the same polynomial expansion in Eq. (13) for the tractions along the crack surface, thus avoiding the troubles of computing stresses or displacements near the crack tip:

$$\begin{cases} K^R \\ K^L \end{cases} = \left\{ c_0 + \frac{1}{2} [\pm c_1 + c_2] + \frac{1 \cdot 3}{2 \cdot 4} [\pm c_3 + c_4] + \dots + \frac{1 \cdot 3 \dots (N_p - 1)}{2 \cdot 4 \dots N_p} [\pm c_{N_p - 1} + c_{N_p}] \right\} \sqrt{\pi a} \tag{14}$$

where  $K^R$  and  $K^L$  represent the SIF at the right and left tips of the crack, respectively.

3. Solution procedures

It is clear that the unknown COD as well as the fictitious tractions of a crack in a multiple-cracked domain are the responses to the structure geometry, the loading profile, the geometries, the quantities and the distributions of cracks, having mutual interactions among them. Hence in the frame work of the eigen COD boundary integral equations, the problem should be solved step by step in an initiative fashion. For the multiple-cracked domain under loadings, the solution procedure consists mainly of four stages in the proposed approach, i.e., the initiation, the iteration, the convergence check and the post process stages.

3.1. The initiation stage

- (i) Initializing all the data related to the domain, boundary conditions and cracks, etc.;
- (ii) Computing all the local Eshelby matrices,  $S_k$ ;
- (iii) Solving the boundary unknowns using the displacement eigen COD boundary Eq. (1) with the prescribed boundary conditions by neglecting tentatively all the cracks in domain (this step is applicable for crack problems in finite domain).
- (iv) Computing the fictitious tractions of all cracks using the traction boundary Eq. (4) by neglecting tentatively all the cracks in domain;

- (v) Computing the initial SIF using Eq. (14) with the fictitious tractions for all cracks;

3.2. Iteration procedures

In this block, the eigen COD of all the cracks are computed sequentially one at a time with the fictitious tractions, consisting of two parts as follows:

- i) The first part is computed using the fictitious tractions of the current crack and cracks in adjacent group via the local Eshelby matrix using Eq. (12);
- ii) The second part is computed by using the fictitious tractions of all the cracks in far-field group excluding those of the current and the adjacent cracks, using a modified traction equation of Eq. (4) as follows:

$$\begin{aligned} \tau_i (y \in A_l^+) = & n_j(y) \int_{\Gamma} \tau_k(x) u_{ijk}^*(x,y) d\Gamma(x) - n_j(y) \int_{\Gamma} u_k(x) \tau_{ijk}^*(x,y) d\Gamma(x) \\ & - n_j(y) \sum_{m=1, m \neq N_l}^{N_c} \int_{A_m^+} \Delta u_k(x) \tau_{ijk}^*(x,y) dA(x), \quad l=1, \dots, N_c \end{aligned} \tag{15}$$

where  $N_l^+$  represents the cracks of adjacent group centered at the current crack  $l$ . Then computing the corresponding SIF of all cracks using Eq. (14);

3.3. Convergence check

The convergence criterion can be chosen as that the maximum difference of the values of SIF between two consecutive computations is no greater than that of prescribed value. Define the maximum iteration error as

$$K_{\max} = \max |K^{(k)} - K^{(k-1)}| \tag{16}$$

which is the maximum difference of the SIF between the two iterations where  $k$  is the number of iteration count. The convergence criterion in the present study is chosen as follows:

$$K_{\max} / \sigma \sqrt{\pi a} \leq 10^{-3} \tag{17}$$

It needs to be pointed out that the expression of Eq. (17) is the non-dimensional SIF normalized by that of the single crack in infinite plate, which can be realized as a kind of relative error to some extent.

- i) If the criterion is not satisfied, solve the boundary unknowns again with the eigen COD of all cracks then return to the previous step (Iteration procedures);
- ii) If the criterion is satisfied, go to the next step (Post processes);

3.4. Post processes

The post processes can be carried out according to the requirements or interests of the research as follows:

- i) Computing the overall properties such as the rigidities, Poisson ratios, anisotropies, etc.;
- ii) Computing the fracture properties combined with the fracture criteria and the maximum SIF computed;
- iii) Investigating the details such as the local stress or strain fields, etc.

The solution procedures of the present approach are summarized in the flow chart as shown in Fig. 3.

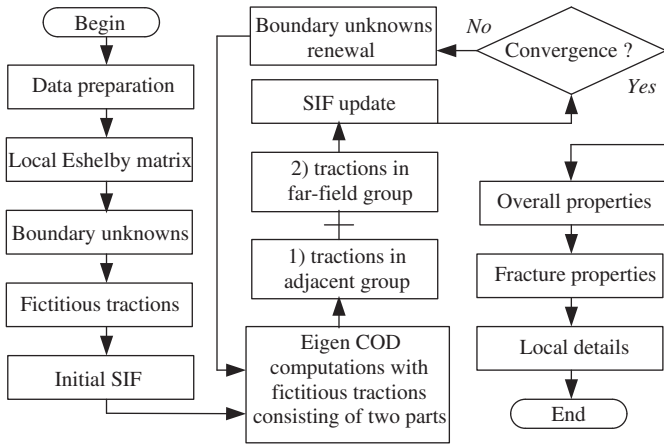


Fig. 3. The flow chart of the solution procedures.

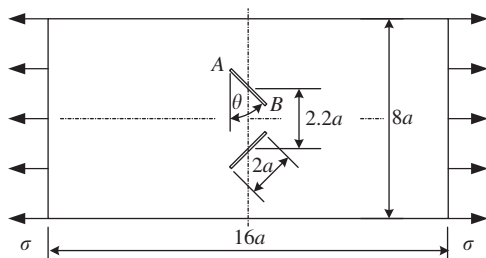


Fig. 4. A plate in tension with two cracks of equal size.

4. Numerical examples

In the numerical examples, the stress intensity factors (SIFs) of the multiple crack problems in the finite and infinite plates are solved with the proposed approach, the eigen-COD boundary integral equations with the iteration procedure (Fig. 3) using the boundary point method (BPM), a discrete form of the BIE [23,24]. The numerical results in the finite plates are compared with those using the dual boundary integral equations (D-BIE) [10,11] and the BIE with the numerical Green's function (NGF) [15,16] and as well as with those in literature. The numerical results in the infinite plates are compared with the analytical solutions in literature. The placement of the nodes along the crack line are chosen as the Chebyshev–Gauss–Lobatto distribution [28] in the D-BIE approach and the Gauss distributions in both of the NGF and the eigen-COD approaches.

4.1. Stress intensity factors in finite plates

4.1.1. A plate with two cracks

The purpose of the first example in finite plates presented is for the verification of the computer programs of the three approaches, the eigen-COD, the D-BIE and the NGF. The plate in tension with two cracks (the total crack number  $N_C=2$ ) of equal size as shown in Fig. 4 was previously analyzed by Chen and Chen [25] using the D-BIE method. In this example, the outer boundary are discretized by using 124 nodes, in all the three approaches. The cracks are discretized by using 17 nodes in the D-BIE and using 13 nodes in both of the NGF and the eigen COD approaches. As there is no analytical results for this example, the results using the most popular D-BIE method serve as the control so that more nodes is used (17 nodes). The number of cracks in adjacent group is set as  $N_L=2$ , the same as that of the total cracks ( $N_L=N_C$ ) in the eigen-COD approach.

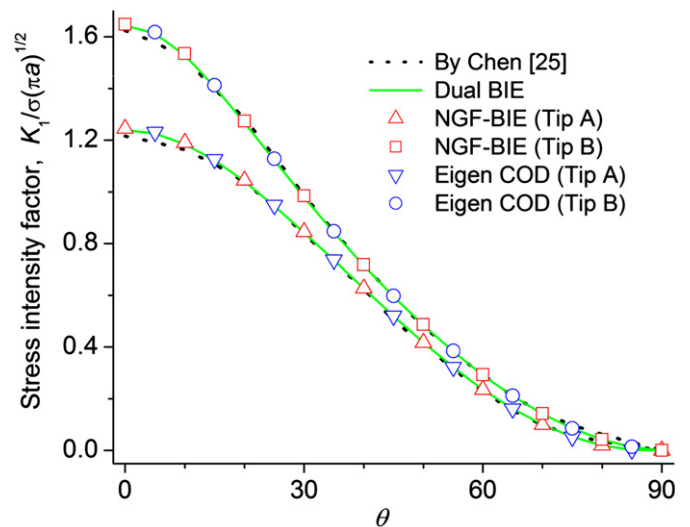


Fig. 5. Normalized mode-I stress intensity factors as a function of tilting angle  $\theta$  for the plate in tension with two cracks.

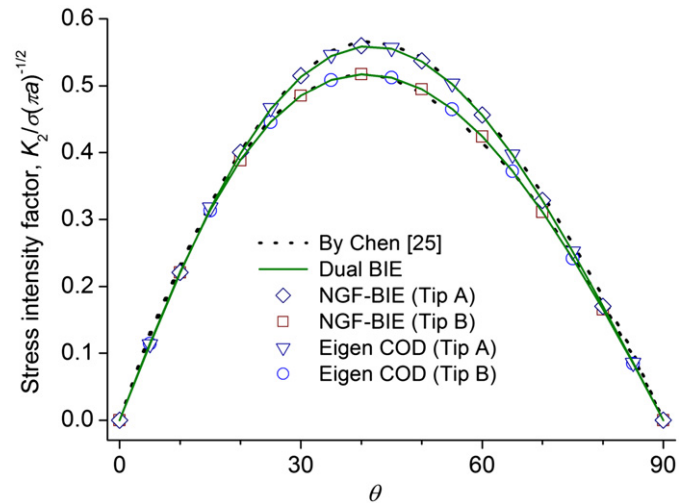


Fig. 6. Normalized mode-II stress intensity factors as a function of angle  $\theta$  for the plate in tension with two cracks.

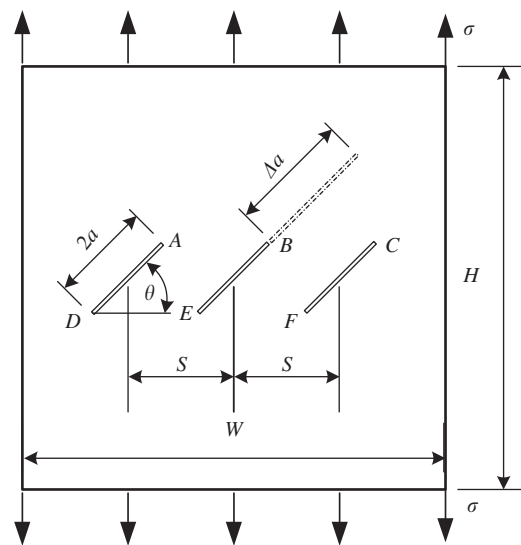


Fig. 7. A square plate in tension with three inclined cracks.

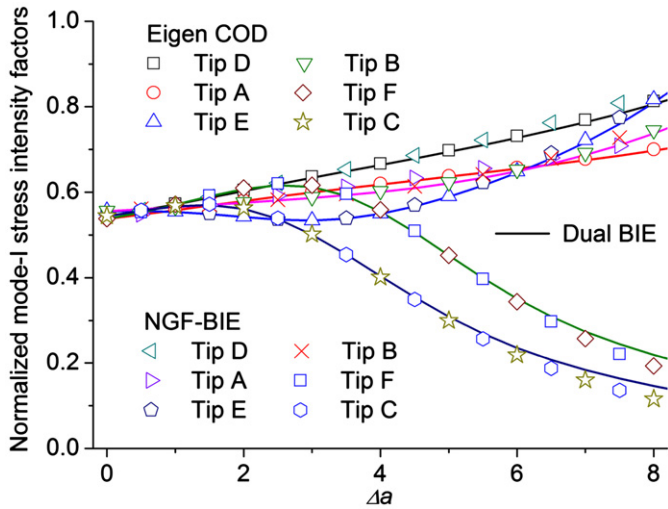


Fig. 8. Normalized mode-I stress intensity factors as a function of crack extension  $\Delta a$  at the tip B of the middle crack for the square plate with three inclined cracks.

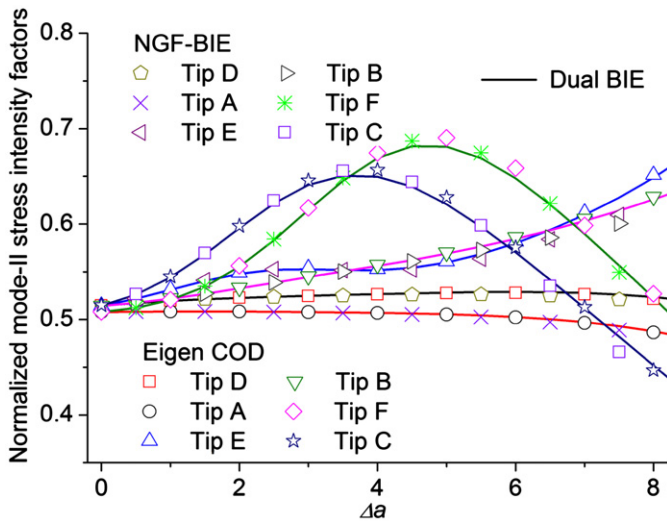


Fig. 9. Normalized mode-II stress intensity factors as a function of crack extension  $\Delta a$  at the tip B of the middle crack for the square plate with three inclined cracks.

Table 1  
The CPU time (s) of the three approaches.

D-BIE	NGF	Eigen COD
20.490	10.561	3.229

The computed mode-I and mode-II stress intensity factors at the crack tips A and B are presented in Figs. 5 and 6, respectively, showing that the computed results of the three algorithms are almost the same with each other and they are all in good agreement with the previous analysis by Chen and Chen [25]. It is seen clearly that the accuracy of the proposed approach has been greatly improved in comparison with the previous work [20]. The effectiveness of the eigen COD BIE is verified.

4.1.2. A plate with three cracks

The second example in finite plates presented is a square plate ( $W=H=20, S=5$ ) in tension with three cracks ( $N_C=3$ ) with the same incline angles  $\theta=45^\circ$  as shown Fig. 7. The half lengths are  $a=1$  for all three cracks at initial stage. The stress intensity factors at the six crack tips are computed when the middle crack extends by  $\Delta a$  at the tip B (Fig. 7) using the three approaches. The outer boundary are discretized by using 200 nodes in all the three approaches. The cracks are discretized by using 21 nodes in the D-BIE and using 13 nodes in both of the NGF and the eigen COD approaches in this example. The number of cracks in adjacent group is set as  $N_L=3$ , the same as that of the total cracks ( $N_L=N_C$ ) in this example in the eigen COD approach.

The computed mode-I and mode-II stress intensity factors at the six crack tips are presented in Figs. 8 and 9, respectively, showing that the computed results of the eigen COD approach are in agreement with the other two approaches, which verifies the proposed approach. It is seen from Fig. 8 that the mode-I stress intensity factors at both of the tips C and F of the right crack (Fig. 7) decrease with the increase of crack extension,  $\Delta a$ , at the tip B of the middle crack, showing the shielding effect of the middle crack on the right crack.

Table 2  
Comparison of the normalized SIF using the three approaches.

$N_C/n$	$\theta$	Algorithm	$K_{1,R}/\sigma\sqrt{\pi a}$	$K_{2,R}/\sigma\sqrt{\pi a}$	$K_{1,L}/\sigma\sqrt{\pi a}$	$K_{2,L}/\sigma\sqrt{\pi a}$
9/3	55.86°	Eigen COD	0.33727	0.46582	0.37067	0.47128
		D-BIE	0.33769	0.46597	0.37127	0.47139
		NGF	0.33831	0.46563	0.36927	0.47109
25/5	-55.75°	Eigen COD	0.34980	-0.42286	0.35284	-0.40689
		D-BIE	0.34882	-0.42564	0.35251	-0.40931
		NGF	0.32567	-0.41479	0.32739	-0.39900
49/7	-83.08°	Eigen COD	0.05480	-0.12166	0.03214	-0.12559
		D-BIE	0.05449	-0.11977	0.03334	-0.12378
		NGF	0.04912	-0.11936	0.02765	-0.12350
81/9	12.20°	Eigen COD	0.95735	0.20245	0.96036	0.19772
		D-BIE	0.95837	0.20377	0.96119	0.19941
		NGF	0.93178	0.19443	0.94492	0.19008
121/11	60.50°	Eigen COD	0.24488	0.40926	0.23208	0.40980
		D-BIE	0.24355	0.41029	0.23128	0.41148
		NGF	0.23939	0.40580	0.22916	0.40616

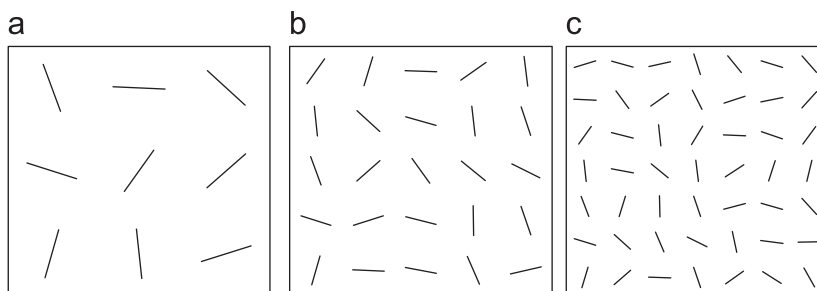


Fig. 10. The square plates in tension with multiple cracks of equal size. (a)  $N_C=9$  (b)  $N_C=25$  (c)  $N_C=49$ .

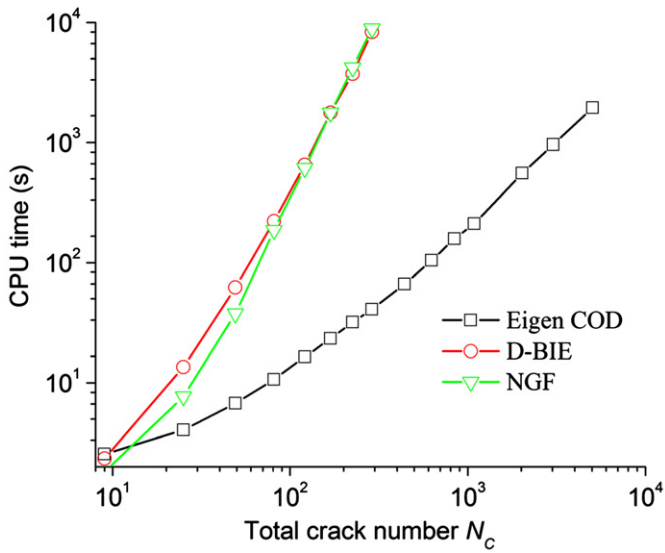


Fig. 11. The CPU time as a function of the total number of cracks,  $N_c$ , for the three approaches.

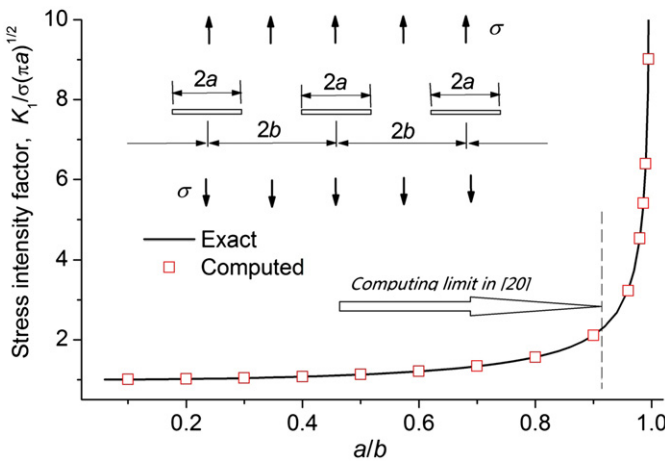


Fig. 12. The normalized stress intensity factors as a function of  $a/b$  for one row of periodical collinear cracks in horizontal line.

It is seen from Fig. 9 that the mode-II stress intensity factors at both of the tips C and F of the right crack (Fig. 7) behave in a more complicated manner with the growth of crack extension,  $\Delta a$ , at the tip B of the middle crack. It is considered that the effect of the interaction between the middle and the right cracks becomes gradually stronger when the crack extension,  $\Delta a$ , is not too large so that the mode-II stress intensity factors increase at both of the tips C and F of the right crack (Fig. 7), but the shielding effect becomes predominant when the size of  $\Delta a$  grows large so that the mode-II stress intensity factors decrease at both the tips C and F of the right crack.

The CPU times of the three approaches, using the desk-top computer Dell with Intel Pentium Dual CPU, 1.60 GHz, are compared in Table 1, showing the high efficiency of the proposed eigen COD algorithm. This is because that the crack unknowns appear in the discrete algebraic equations in the D-BIE algorithm, resulting in a greater size of the system matrix. In contrast, the crack unknowns do not appear in the discrete algebraic equations in both of the NGF and the eigen COD approaches, resulting in relatively smaller sizes of the system matrices. In the NGF approach, however, the complementary function need to be solved numerically and embedded in the NGF to modify the

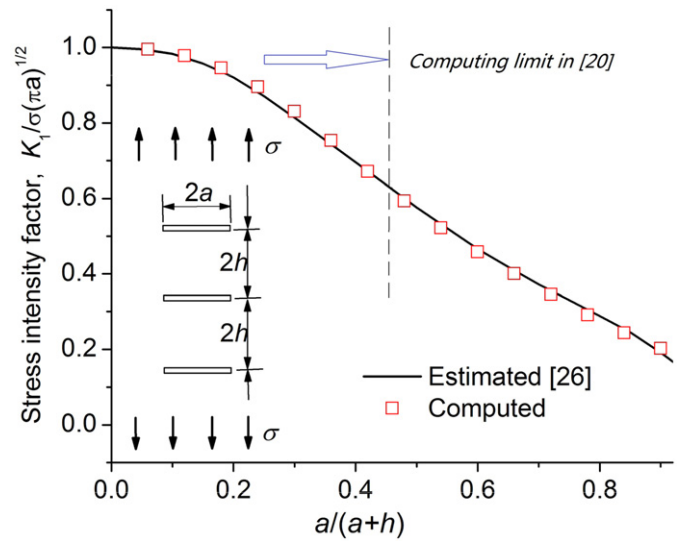


Fig. 14. The normalized stress intensity factors as a function of  $a/(a+h)$  for one column of periodical cracks in vertical line.

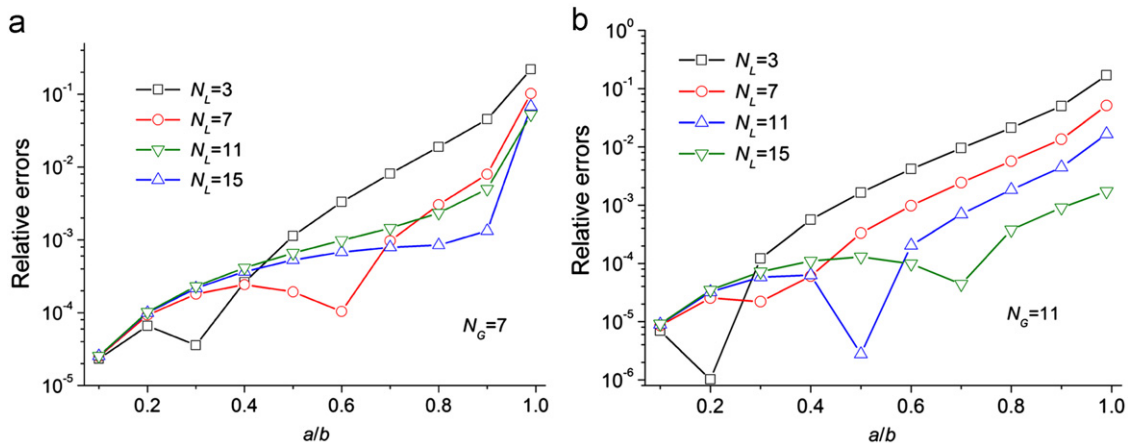


Fig. 13. The relative errors of SIF as a function of  $a/b$  using different number of cracks in adjacent group with Gauss point numbers,  $N_G=7$  (a) and  $N_G=11$  (b).

entries of the system matrix. While the system matrix is remained the same in the iteration process in the eigen COD approach and the convergence can be reached generally by 3–4 iterations so that the efficiency of the eigen COD approach is higher than that of the NGF approach. This example verifies the effectiveness of the eigen COD approach.

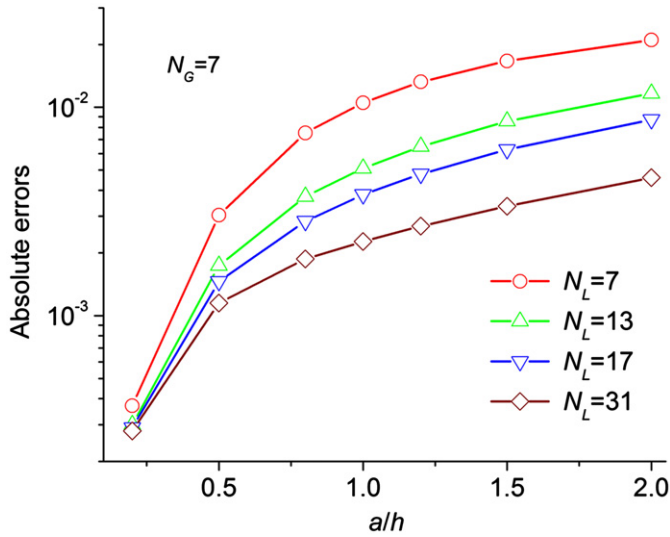


Fig. 15. The absolute errors of SIF as a function of  $a/h$  using different number of cracks in adjacent group with Gauss point numbers,  $N_G=7$ .

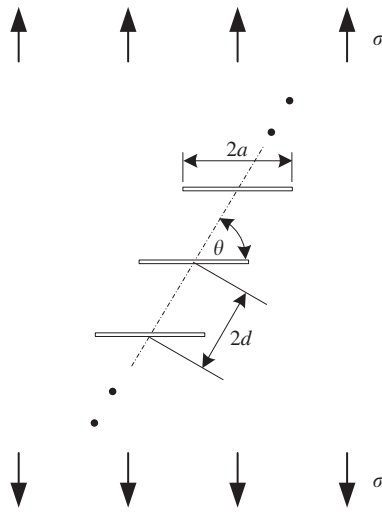


Fig. 16. One row of echelon cracks with length  $2a$  and spacing  $2d$  under a uniform far-field tension  $\sigma$  perpendicular to the crack faces.

Table 3  
The normalized SIF of one row of echelon cracks (Fig. 16).

$\theta$	$a/d=0.5$				$a/d=1.0$			
	$K_I/\sigma\sqrt{\pi a}$		$K_{II}/\sigma\sqrt{\pi a}$		$K_I/\sigma\sqrt{\pi a}$		$K_{II}/\sigma\sqrt{\pi a}$	
	Ref. [30]	Computed	Ref. [30]	Computed	Ref. [30]	Computed	Ref. [30]	Computed
15	1.1685	1.1686	0.0473	0.0473	2.7947	2.7588	-0.3258	-0.3279
30	1.1822	1.1823	-0.0230	-0.0230	1.7666	1.7525	-0.4705	-0.4674
45	1.0919	1.0918	-0.1182	-0.1183	1.2115	1.2064	-0.4769	-0.4746
60	0.9509	0.9507	-0.1477	-0.1479	0.8521	0.8500	-0.3796	-0.3790
75	0.8340	0.8335	-0.0979	-0.0981	0.6407	0.6389	-0.2090	-0.2091

#### 4.1.3. A plate with multiple cracks

The third example in finite plates presented are the square plates in tension with multiple cracks, some of them as shown in Fig. 10. The total number of cracks are chosen as  $N_C=(2n+1)^2$ ,  $n=1,2,\dots$ , where  $n$  is an integer. The size of each crack is taken as  $2a=0.4W/n$ , where  $W=H$  are the width and the height of the plate, respectively. The Gauss point number used is  $N_G=13$ . The orientation of the cracks are generated using the random function in the computer program. The stress intensity factors of the crack at the center of the plate are computed by using the three approaches. The number of cracks in adjacent group is set as  $N_L=9$  in the eigen COD approach.

The stress intensity factors of the crack at the plate center are listed and compared in Table 2 among the three approaches with the total crack number  $N_C=9, 25, 49, 81$  and  $121$ , showing that the results of the proposed approach are in agreement with the D-BIE and the NGF approaches, verifying the effectiveness of the proposed eigen COD approach.

The CPU time are compared in Fig. 11 for the three approaches, where the maximum total crack numbers are 289 for the D-BIE and the NGF approaches, respectively, but in contrast, the maximum total cracks computed is 5041 for eigen COD approach. Fig. 11 shows that the efficiency of the proposed eigen COD approach is much higher than that of the other two approaches when the total number of cracks grows larger. This is because, as mentioned previously, the size of the system matrix of the D-BIE approach increases with the total crack number, while the sizes of the system matrices of either the NGF or the eigen COD approaches remain unchanged. However, in the NGF approach, the size of the matrix to determine the complementary solution for the NGF increases also with the total crack number. Much computing time is required for solving this matrix for the complementary solution. In addition, after their solution, the complementary functions, need to be embedded into the system matrix to modify the entries of it, also taking much computing time, showing that in view of the computational efficiency, the NGF approach is no better than that of the D-BIE approach in the case of a large number of cracks. However, from the computational point of view, solving a problem with many small matrices, which is just the case of the eigen-COD approach, would be much efficient than that of solving a single huge matrix, which are the cases of the D-BIE and the NGF approaches. More the number of cracks involved, much greater the difference of efficiencies between the two problems will be, which is the main factor resulting in the high efficiency of the proposed approach.

#### 4.2. Stress intensity factors in infinite plates

##### 4.2.1. One row of periodical collinear cracks in horizontal line

The first example in infinite plates presented is a row of periodic equal cracks under a far-field tension perpendicular to

the crack faces. In the computation, up to 2001 cracks ( $N_C=2001$ ) are taken into consideration instead of using the infinite number of cracks. The normalized stress intensity factors of crack tip are calculated by the proposed approach and by the analytic solution of Sih [29] are compared in Fig. 12, showing a good agreement between the numerical and the analytical solutions. A dashed line given in Fig. 12 is the computing limit, that over this limit, no reasonable result can be obtained in the previous work [20] because of the interaction among cracks. However, with the local Eshelby matrix being introduced in the present work, the treatment of the interaction among cracks has been greatly improved.

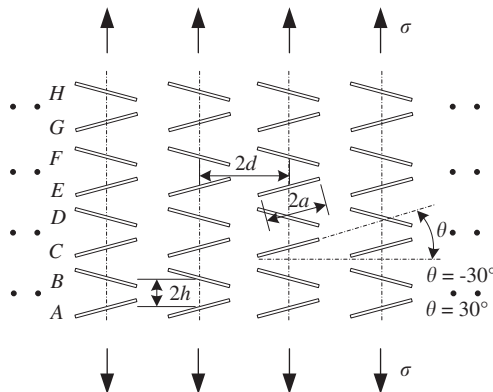


Fig. 17. The eight rows of periodical cracks with different decline angles.

The relative errors of SIF as a function of  $a/b$  are presented in Fig. 13 with different number of cracks in adjacent group,  $N_L$ , using Gauss point numbers,  $N_C=7$  (a) and  $N_C=11$  (b), respectively. It can be seen that in general, the increase of the Gauss point numbers can increase the accuracy of the numerical results. The interactions among cracks increase with the ration of  $a/b$ , the effects of which can be compensated by increasing the number of cracks in adjacent group so that the cost increases correspondingly.

4.2.2. One column of periodical cracks in vertical line

The second example in infinite plates presented is a column of periodic equal cracks in vertical line under a far-field tension perpendicular to the crack faces. In the computation, up to 2001 cracks ( $N_C=2001$ ) are taken into consideration instead of using the infinite number of cracks. The normalized stress intensity factors of crack tip are calculated by the proposed approach and by the estimated solution of Tada et al. [26] are compared in Fig. 14, showing also a good agreement between the numerical and the estimated solutions. A dashed line given in Fig. 14 is also the computing limit, that over this limit, no reasonable result can be obtained in the previous work [20] because of the interaction among cracks. However, with the local Eshelby matrix being introduced in the present work, the treatment of the interaction among cracks has been greatly improved.

Taking the tabulated data by Wang [30] for one column of periodical cracks in vertical line as the control, the absolute errors of SIF as a function of  $a/h$  are presented in Fig. 15 with different

Table 4 Normalized SIF of cracks in line A (Fig. 17,  $h/d=0.5$ ,  $N_L=8$ ,  $N_C=13$ ).

$a/d$	$K_{1,L}/\sigma\sqrt{\pi a}$		$K_{1,R}/\sigma\sqrt{\pi a}$		$K_{2,L}/\sigma\sqrt{\pi a}$		$K_{2,R}/\sigma\sqrt{\pi a}$	
	Ref. [30]	Computed						
0.5	0.8488	0.8484	0.7350	0.7344	0.3668	0.3666	0.4345	0.4343
0.6	0.9228	0.9225	0.7645	0.7639	0.3709	0.3708	0.4703	0.4701
0.7	1.0200	1.0195	0.8105	0.8094	0.3960	0.3958	0.5329	0.5323
0.8	1.1362	1.1356	0.8612	0.8590	0.4504	0.4501	0.6315	0.6307
0.9	1.2618	1.2616	0.8874	0.8813	0.5375	0.5388	0.7792	0.7783

Table 5 Normalized SIF of cracks in line B (Fig. 17,  $h/d=0.5$ ,  $N_L=8$ ,  $N_C=13$ ).

$a/d$	$K_{1,L}/\sigma\sqrt{\pi a}$		$K_{1,R}/\sigma\sqrt{\pi a}$		$K_{2,L}/\sigma\sqrt{\pi a}$		$K_{2,R}/\sigma\sqrt{\pi a}$	
	Ref. [30]	Computed						
0.5	0.6779	0.6772	0.6771	0.6763	-0.3743	-0.3739	-0.3850	-0.3847
0.6	0.6924	0.6916	0.6886	0.6878	-0.4006	-0.4003	-0.4189	-0.4185
0.7	0.7193	0.7179	0.7104	0.7090	-0.4549	-0.4542	-0.4830	-0.4823
0.8	0.7445	0.7424	0.7260	0.7237	-0.5443	-0.5432	-0.5854	-0.5842
0.9	0.7299	0.7253	0.6874	0.6840	-0.6799	-0.6805	-0.7405	-0.7408

Table 6 Normalized SIF of cracks in line C (Fig. 17,  $h/d=0.5$ ,  $N_L=8$ ,  $N_C=13$ ).

$a/d$	$K_{1,L}/\sigma\sqrt{\pi a}$		$K_{1,R}/\sigma\sqrt{\pi a}$		$K_{2,L}/\sigma\sqrt{\pi a}$		$K_{2,R}/\sigma\sqrt{\pi a}$	
	Ref. [30]	Computed						
0.5	0.6858	0.6851	0.6862	0.6855	0.3758	0.3754	0.3774	0.3770
0.6	0.7042	0.7034	0.7044	0.7036	0.4040	0.4037	0.4069	0.4065
0.7	0.7352	0.7345	0.7354	0.7340	0.4602	0.4595	0.4649	0.4642
0.8	0.7685	0.7664	0.7662	0.7640	0.5514	0.5503	0.5589	0.5578
0.9	0.7715	0.7662	0.7632	0.7581	0.6881	0.6885	0.7010	0.7014

number of cracks in adjacent group,  $N_L$ , using Gauss point number,  $N_G=7$ . It can be seen that the interactions among cracks increase with the ratio of  $a/h$ , the effects of which can be compensated by increasing the number of cracks in adjacent group so that the cost increases correspondingly. It is noticed by comparing Fig. 14 and Fig. 12 that the interactions among cracks arranged in parallel side by side in a column vertical line are stronger than those of cracks arranged in a collinear row of horizontal line.

4.2.3. One row of periodical echelon cracks

The third example presented is the common case of single periodic cracks, the one row of echelon cracks in an infinite plate under a far-field tension stress  $\sigma$  perpendicular to the crack surfaces as shown in Fig. 16. In the computation, up to 2001 cracks ( $N_C=2001$ ) are taken into consideration instead of using the infinite number of cracks. The normalized stress intensity factors of crack tip are calculated by the proposed approach in comparison with those by Wang [30] as listed in Table 3 where the agreement between the two can be seen.

4.2.4. Eight rows of periodical cracks with different decline angles

The fourth example presented is the eight rows of periodical cracks with different decline angles in an infinite plate under a far-field tension stress in vertical direction as shown in Fig. 17. In the computation, up to 16008 cracks ( $N_C=16008$ ) are taken into consideration instead of using the infinite number of cracks. The normalized stress intensity factors of crack tip in the lines A, B, C and D are calculated by the proposed approach in comparison with those by Wang [30] as listed in Table 4 through 7 where the agreement between the two can also be seen. Tables 5–7

The absolute errors of SIF as well as the CPU time are presented in Fig. 18 for the eight rows of periodical cracks with different decline angles as a function of total crack number,  $N_C$ , showing that the errors decrease monotonically to an acceptable level with the increase of the total crack number,  $N_C$ , for the infinite cracks in infinite plate. The CPU time increases almost linearly with the number of  $N_C$  when  $N_C$  is large, showing the high efficiency of the proposed approach.

4.2.5. One row of periodical two-crack groups in an inclined position

The fifth example presented is the one row of periodical two-crack groups in an inclined position under a far-field tension stress in vertical direction in infinite plate as shown in Fig. 19. In the computation, up to 4002 cracks ( $N_C=4002$ ) are taken into consideration instead of using the infinite number of cracks. The number of Gauss points used is chosen as  $N_G=9$  and the number of cracks in adjacent group is chosen as  $N_L=10$  in the computation. The normalized stress intensity factors at the crack tips A, B, C and D (Fig. 19) are calculated by the proposed approach in comparison with those by Chen [31] as shown in Fig. 20. It is seen from Fig. 20 that the computed results are in good agreement with those by Chen [31], verifying the effectiveness and the accuracy of the proposed approach.

4.2.6. One row of periodical two-crack groups in a stacked position

The sixth example presented is the one row periodical two-crack groups in a stacked position under a far-field tension stress in vertical direction in infinite plate as shown in Fig. 21 where  $2a/d=0.9$  is used. In the computation, up to 4002 cracks ( $N_C=4002$ ) are taken into consideration instead of using the infinite number of cracks. The number of Gauss points used is chosen as  $N_G=7$  and

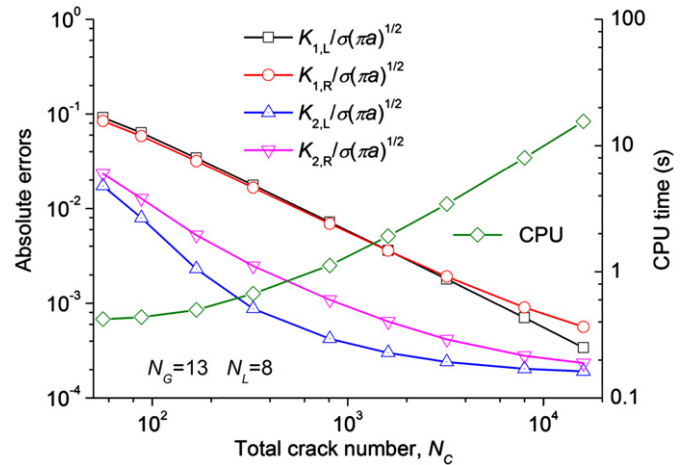


Fig. 18. The absolute errors of SIF in eight rows of periodical cracks with different decline angles as a function of total crack number,  $N_C$  (Fig. 17).

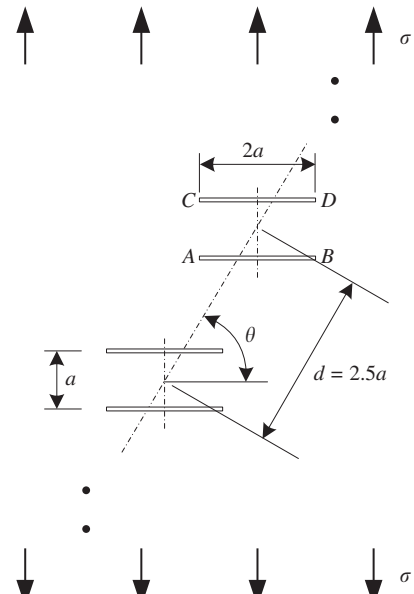


Fig. 19. The one row of periodic two-crack groups in an inclined position.

Table 7  
Normalized SIF of cracks in line D (Fig. 17,  $h/d=0.5$ ,  $N_L=8$ ,  $N_C=13$ ).

$a/d$	$K_{1,L}/\sigma\sqrt{\pi a}$		$K_{2,L}/\sigma\sqrt{\pi a}$		$K_{2,L}/\sigma\sqrt{\pi a}$		$K_{2,R}/\sigma\sqrt{\pi a}$	
	Ref. [30]	Computed						
0.5	0.6851	0.6843	0.6851	0.6844	-0.3770	-0.3767	-0.3773	-0.3769
0.6	0.7026	0.7018	0.7027	0.7019	-0.4061	-0.4057	-0.4066	-0.4062
0.7	0.7329	0.7314	0.7329	0.7314	-0.4633	-0.4626	-0.4642	-0.4635
0.8	0.7626	0.7603	0.7622	0.7598	-0.5562	-0.5550	-0.5578	-0.5566
0.9	0.7570	0.7520	0.7549	0.7500	-0.6962	-0.6966	-0.6994	-0.6999

the number of cracks in adjacent group is chosen as  $N_L=14$  in the computation. The normalized stress intensity factors in the modes I and II at the crack tips A, B, C and D (Fig. 21) are calculated by the proposed approach in comparison with those by Chen [31] as shown in Figs. 22 and 23, respectively. It is seen from both of Figs. 22 and 23 that the computed results are in good agreement

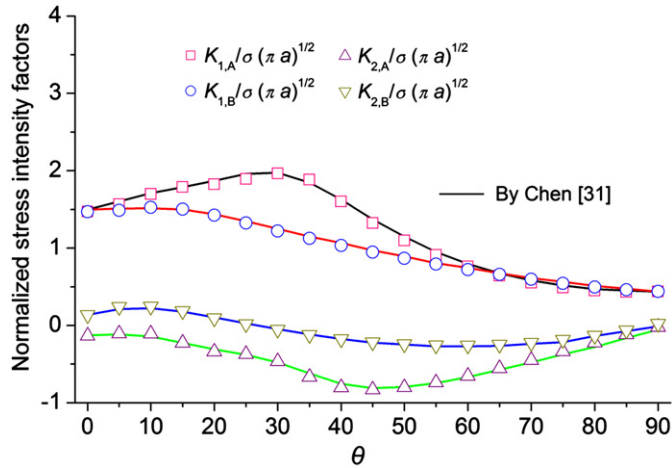


Fig. 20. The normalized SIF for one row of periodic two-crack groups in an inclined position (Fig. 19).

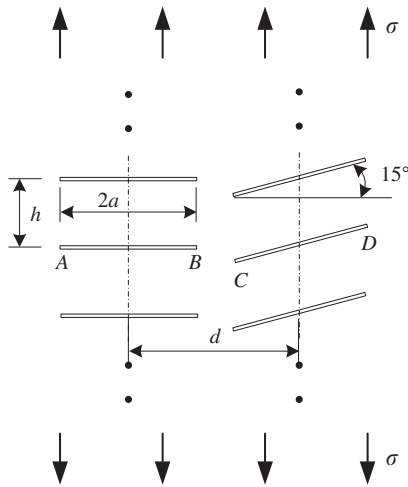


Fig. 21. The one row of periodical two-crack groups in a stacked position.

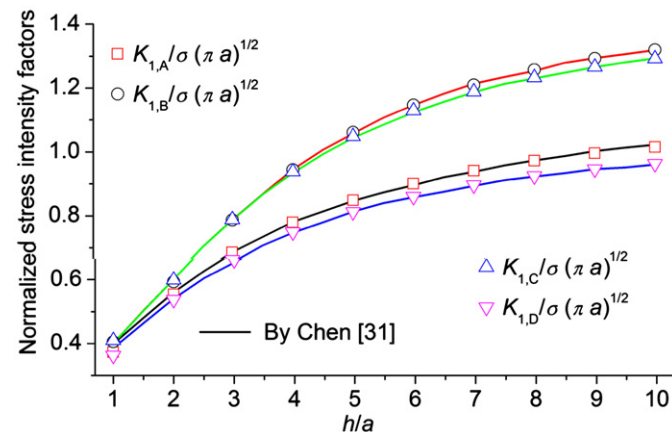


Fig. 22. The mode I normalized SIF for one row of periodical two-crack groups in a stacked position (Fig. 21).

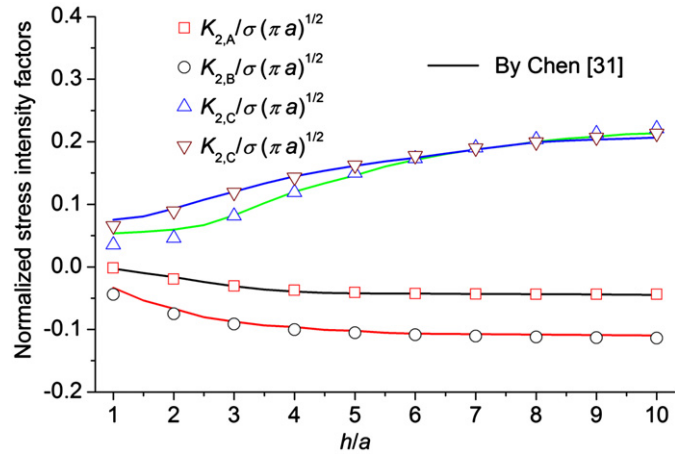


Fig. 23. The mode II normalized SIF for one row of periodical two-crack groups in a stacked position (Fig. 21).

with those by Chen [31], verifying again the effectiveness and accuracy of the proposed approach.

### 5. Conclusion

A newly developed computational approach based on the eigen COD BIEs is proposed for the analysis of elastic solids with large number of cracks. The eigen COD is defined as the crack opening displacement of a crack in infinite domain under the fictitious traction acting on the crack surface. With this approach, the multiple crack problem is solved by using the conventional displacement discontinuity BIE in an iterative fashion to determine all the unknown CODs step by step with a small size of system matrix. The interactions among cracks are dealt with by two parts according to the distances of cracks to the current crack. The strong effects of cracks in adjacent group were treated with the aid of the local Eshelby matrix derived from the traction BIEs in discrete form. While the relatively weak effects of cracks in far-field group were treated in the iteration procedures. The effectiveness and the accuracy of the proposed approach were verified by computing the stress intensity factors in a number of numerical examples of cracks, up to several thousands in number, in both the finite and infinite plates with regard to the accuracies and efficiencies with those by the other numerical approaches of the D-BIE and the NGF as well as the analytical solutions in the literature.

### Acknowledgements

The support of the National Natural Science Foundation of China (11272195, 10972131, 11172159) and the Australian Research Council (LP0990514) are gratefully acknowledged

### Appendix A

The concept of the eigen crack opening displacements (COD) are firstly introduced in [20] in the form of Eq. (1), the displacement BIE with the displacement discontinuities, or the COD on crack surfaces [15,16,25]. In addition to the conventional derivation of the displacement BIE, however, the crack integral, the last term in Eq. (1) correlates intimately with the domain integral in the formulation of eigen-strain BIEs [21,22], from which the

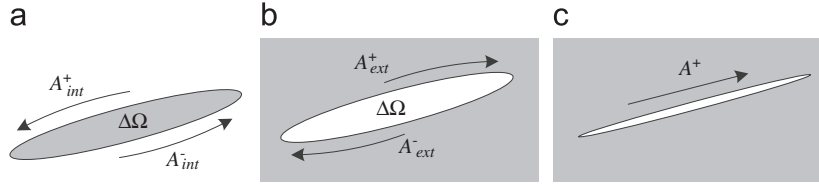


**Fig. A1.** Schematics of the correlation between the eigen COD and the eigenstrain. (a) A narrow shape as an interior problem; (b) The corresponding exterior problem; (c) The limit process when the shortest dimension reducing to zero.

terminology eigen COD comes:

$$\begin{aligned} \gamma u_i(y) &= \int_{\Gamma} \tau_j(x) u_{ij}^*(x,y) d\Gamma(x) - \int_{\Gamma} u_j(x) \tau_{ij}^*(x,y) d\Gamma(x) \\ &\quad - \sum_{I=1}^{N_I} \int_{\Delta\Omega_I} \varepsilon_{jk}^0(x) \sigma_{ijk}^*(x,y) d\Omega(x), \end{aligned} \tag{A1}$$

where  $\varepsilon_{jk}^0$  are the eigenstrains in the sub-domain  $\Delta\Omega$ ,  $N_I$  the total number of the inhomogeneity. Now consider only the domain integral of one single inhomogeneity with a narrow shape in an infinite medium, occupying the sub-domain  $\Delta\Omega$  with the boundary  $A_{int} = A_{int}^+ \cup A_{int}^-$  as an interior problem as shown in Fig. A1(a).

$$I = \int_{\Delta\Omega} \varepsilon_{jk}^0(x) \sigma_{ijk}^*(x,y) d\Omega(x) \tag{A2}$$

Suppose that the elastic modulus of the inhomogeneity is zero, i.e., the empty hole. Employing the geometric relation between strains and displacements and using the Gaussian divergence theorem, the domain integral becomes

$$\begin{aligned} I &= \frac{1}{2} \int_{\Delta\Omega} [u_{j,k}^0(x) + u_{k,j}^0(x)] \sigma_{ijk}^*(x,y) d\Omega(x) \\ &= \frac{1}{2} \int_{A_{int}} (u_j^0 n_k + u_k^0 n_j) \sigma_{ijk}^* dA(x) - \frac{1}{2} \int_{\Delta\Omega} (u_j^0 \sigma_{ijk}^* + u_k^0 \sigma_{ijk}^*) d\Omega(x) \end{aligned} \tag{A3}$$

where  $u_j^0$  are the displacements corresponding to the eigenstrain  $\varepsilon_{jk}^0$ ,  $n_k$  the unit outward normal. With the Cauchy relation  $\tau_{ij}^* = \sigma_{ijk}^* n_k$  and noticed that the second integral above in Eq. (A3) should be zero since  $\sigma_{ijk}^* = \sigma_{ijk}^* = 0$ , so that

$$I = \int_{A_{int}} u_j^0(x) \tau_{ij}^*(x,y) dA(x) \tag{A4}$$

Decomposing the boundary into the upper and lower parts by  $A_{int} = A_{int}^+ \cup A_{int}^-$  and using the relation  $\tau_{ij}^*(x,y)|_{y \in \Delta A_{int}^+} = -\tau_{ij}^*(x,y)|_{y \in \Delta A_{int}^-}$  when taking a limit process of  $\Delta\Omega \rightarrow 0$  by letting the shortest dimension of the narrow hole reduce to zero, the integral becomes

$$\begin{aligned} I &= \int_{A_{int}^+} u_j^+(x) \tau_{ij}^*(x,y) dA(x) + \int_{A_{int}^-} u_j^-(x) \tau_{ij}^*(x,y) dA(x) \\ &= \int_{A_{int}^+} (u_j^+ - u_j^-) \tau_{ij}^*(x,y) dA(x) \\ &= \int_{A_{int}^+} \Delta u_j(x) \tau_{ij}^*(x,y) dA(x) \end{aligned} \tag{A5}$$

where  $\Delta u_k$  is the eigen-COD computed by  $\Delta u_k = u_k^+ - u_k^-$ ,  $u_k^+$  and  $u_k^-$  being the displacements on the upper and the lower boundaries,  $A_{int}^+$  and  $A_{int}^-$ , respectively. The interior problem can be changed equivalently to the corresponding exterior problem as shown in Fig. A1(b):

$$I = - \int_{A_{ext}^+} \Delta u_j(x) \tau_{ij}^*(x,y) dA(x) \tag{A6}$$

Finally after taking the limit process  $\Delta\Omega \rightarrow 0$  by letting the shortest dimension of the narrow hole reduce to zero as shown in Fig. A1(c), the original domain integral can be written as a crack

integral along the crack line with the eigen-COD,  $\Delta u_k$ , expressed in concise form as follows

$$I = - \int_{A^+} \Delta u_j(x) \tau_{ij}^*(x,y) dA(x) \tag{A7}$$

In this way, for an elastic domain  $\Omega$  with boundary  $\Gamma$  containing multiple cracks, the formulation of eigen-COD BIE (Eq. (1)) can be derived directly from the eigen-strain BIE (Eq. (Aa)) containing multiple zero-modulus inhomogeneities.

**References**

- [1] Dolado JS, Breugel KV. Recent advances in modeling for cementitious materials. *Cem Concr Res* 2011;41:711–26.
- [2] Sobelman OS, Gibeling JC, Stover SM, Hazelwood SJ, Yeh OC, Shelton DR, et al. Do microcracks decrease or increase fatigue resistance in cortical bone? *J Biomech* 2004;37:1295–303.
- [3] Dhanasekar M, Han JJ, Qin QH. Interaction of surface and cracks in railhead. *CAMES* 2007;14:79–89.
- [4] Chen JH, Wang GZ, Yan C, Ma H, Zhu L. Advances in the mechanism of cleavage fracture of low alloy steel at low temperature. Part II: fracture model. *Int J Fract* 1997;83:121–38.
- [5] Chen YZ. Integral equation methods for multiple crack problems and related topics. *Appl Mech Rev* 2007;60:172–94.
- [6] Brebbia CA, Telles JCF, Wrobel LC. *Boundary element techniques—theory and applications in engineering*. Berlin: Springer; 1984.
- [7] Saez A, Gallego R, Dominguez J. Hypersingular quarter-point boundary elements for crack problems. *Int J Numer Methods Eng* 1995;38:1681–701.
- [8] Blandford GE, Ingraffea AR, Liggett JA. Two-dimensional stress intensity factor computation using the boundary element method. *Int J Numer Methods Eng* 1981;17:387–404.
- [9] Aliabadi MH. Boundary element formulations in fracture mechanics. *Appl Mech Rev* 1997;50(2):83–96.
- [10] Chen JT, Hong HK. Review of dual boundary element methods with emphasis on hypersingular integrals and divergent series. *Appl Mech Rev* 1999;52(1) 17–33.
- [11] Portela A, Aliabadi MH, Rooke DP. Dual boundary elements analysis of cracked plates: singularity subtraction technique. *Int J Fract* 1992;55:17–28.
- [12] Greengard LF, Rokhlin V. A fast algorithm for particle simulations. *J Comput Phys* 1987;73:325–48.
- [13] Liu YJ. *Fast multipole boundary element method-theory and applications in engineering*. London: Cambridge University Press; 2009.
- [14] Ang WT, Clements DL. A boundary integral equation method for the solution of a class of crack problems. *J Elast* 1987;17:9–21.
- [15] Telles JCF, Castor GS, Guimaraes S. A numerical Green's function approach for boundary elements applied to fracture mechanics. *Int J Numer Methods Eng* 1995;38:3259–74.
- [16] Telles JCF, Guimaraes S. Green's function: a numerical generation for fracture mechanics problems via boundary elements. *Comput Meth Appl Mech Eng* 2000;188:847–58.
- [17] Kachanov M. Elastic solids with many cracks: a simple method of analysis. *Int J Solids Struct* 1987;23(1):2343.
- [18] Kachanov M. Elastic solids with many cracks and related problems. *Adv Appl Mech* 1993;30:259–445.
- [19] Feng XQ, Yu SW. Damage micromechanics for constitutive relations and failure of microcracked quasi-brittle materials. *Int J Damage Mech* 2010;19: 911–48.
- [20] Guo Z, Ma H. Solution of stress intensity factors of multiple cracks in plane elasticity with eigen COD formulation of boundary integral equation. *J Shanghai Univ* 2011;15(3):173–9.
- [21] Ma H, Yan C, Qin QH. Eigenstrain formulation of boundary integral equations for modeling particle-reinforced composites. *Eng Anal Boundary Elem* 2009; 33(3):410–9.
- [22] Ma H, Fang JB, Qin QH. Simulation of ellipsoidal particle-reinforced materials with eigenstrain formulation of 3D BIE. *Adv Eng Software* 2011;42(10) 750–9.

- [23] Ma H, Qin QH. Solving potential problems by a boundary-type meshless method—the boundary point method based on BIE. *Eng Anal Boundary Elem* 2007;31(9):749–61.
- [24] Ma H, Zhou J, Qin QH. Boundary point method for linear elasticity using constant and quadratic moving elements. *Adv Eng Software* 2010;41(3):480–8.
- [25] Chen WH, Chen TC. An efficient dual boundary element technique for a two-dimensional fracture problem with multiple cracks. *Int J Numer Methods Eng* 1995;38:1739–56.
- [26] Tada H, Paris P, Irwin G. *The stress analysis of cracks handbook*. Suffolk: Professional Engineering Publishers; 1985.
- [27] Hui CY, Shia D. Evaluations of hypersingular integrals using Gaussian Quadrature. *Int J Numer Methods Eng* 1999;44:205–14.
- [28] Bert CW, Malik M. *Differential quadrature method in computational mechanics: a review*. Appl Mech Rev 1996;49:1–27.
- [29] Sih GC. *Handbook of stress intensity factors*. Bethlehem: Lehigh University; 1973.
- [30] Wang GS, Feng XT. The interaction of multiple rows of periodical cracks. *Int J Fract* 2001;110:73–100.
- [31] Chen YZ, Lin XY. Periodic group crack problems in an infinite plate. *Int J Solids Struct* 2005;42:2837–50.